International Journal of Environmental Sciences
ISSN: 2229-7359
Vol. 11 No. 9s, 2025
https://www.theaspd.com/ijes.php

Development And Evaluation Of A Phytosomal Cream Containing Green Synthesized Gold Nanoparticles For The Management Of Air Pollution-Induced Inflammatory Skin Disorders

Jyothirmayee Devineni[1], Rohini Armo[2], Rashmi Mohapatra[3*], Sabnam Nargis[4], Ramesh R. Pagore[5], Ashutosh Pathak[6], Nilkamal Waghmare[7], Lakshmi[8],
[1]Department of Pharmaceutics and Biotechnology, KVSR Siddhartha College of Pharmaceutical Sciences Vijayawada Andhra Pradesh India Pin 520010.
[2]Department of Pharmaceutical Chemistry, Shri Rawatpura sarkar institute of pharmacy, kumhari, Durg Chhattisgarh, India Pin- 490042.
[3]Head, Centre for Indigenous Knowledge on Herbal Medicines and Therapeutics, Kalinga Institute of Social Sciences (KISS), Deemed to be University, Bhubaneswar, Odisha - 751024. India.
[4]Department -Pharmaceutical Chemistry, The Assam Royal Global University, Guwahati, Assam Pincode-781035.
[5]Anuradha college of Pharmacy, Chikhli 443201.
[6]Department of Pharmacy Practice, Teerthanker Mahaveer College of Pharmacy, Teerthanker Mahaveer University, Moradabad UP, India Pin- 244001.
[7]Department of Pharmaceutics, Bharati Vidyapeeth's College of Pharmacy, Navi Mumbai – 400614.
[8]Department of Pharmaceutics, KIET School of Pharmacy, KIET Group of Institutions, Delhi - NCR, Ghaziabad Pin 201206.
*Corresponding Author
Rashmi Mohapatra[3*]
Head, Centre for Indigenous Knowledge on Herbal Medicines and Therapeutics, Kalinga Institute of Social Sciences (KISS), Deemed to be University, Bhubaneswar, Odisha - 751024. India.
Email: rashmi.mohapatra@kiss.ac.in

Abstract
This study focused on the green synthesis of gold nanoparticles (AuNPs) using *Curcuma longa* extract and their integration with phytosome-based vesicular systems to develop a novel antioxidant and anti-inflammatory topical cream. Gold nanoparticles synthesized via varying concentrations of *C. longa* demonstrated a decrease in particle size and polydispersity with increasing extract volume, indicating effective capping and stabilization by phytoconstituents. Phytosomes were prepared using thin-film hydration with different extract-to-phospholipid ratios. PHY-3 (1:3) showed the most favorable properties with the smallest particle size (212.4 nm), highest entrapment efficiency (84.2%), and good stability. These phytosomes, when incorporated into creams with AuNPs, produced formulations (PC-1 to PC-3) exhibiting acceptable pH, increased viscosity, and improved spreadability, with PC-3 being the most optimized. In vitro studies demonstrated dose-dependent antioxidant activity, with PC-3 showing the highest DPPH inhibition (87.9%) and an IC_{50} of 0.30%. Similarly, the protein denaturation assay revealed strong anti-inflammatory activity, with PC-3 exhibiting 84.3% inhibition and an IC_{50} of 0.14%. The findings support the synergistic benefits of combining phytosomes and green-synthesized AuNPs in topical delivery systems, suggesting their promising application in skin protection against oxidative stress and inflammation. Further studies are warranted to validate their safety, efficacy, and long-term stability
Keywords: *Curcuma longa*, Phytosomes, Gold nanoparticles (AuNPs), Green synthesis, *Curcuma longa*, Topical formulation, Anti-inflammatory activity, Antioxidant activity, Air pollution-induced skin damage, Sustainable nanotechnology, Herbal nanocosmeceuticals, Protein denaturation assay.

INTRODUCTION

Skin, the largest organ of the human body, serves as the first line of defense against environmental stressors such as ultraviolet (UV) radiation, pollution, and microbial invasion. Chronic exposure to these stressors often results in oxidative damage and inflammatory responses, contributing to premature aging, pigmentation disorders, and various dermal pathologies. As awareness of the impact of oxidative stress on skin health grows, the demand for topical formulations enriched with antioxidants and anti-inflammatory agents has surged. However, conventional formulations frequently suffer from poor bioavailability, limited skin penetration, and instability of active ingredients. To overcome these challenges, innovative drug delivery systems such as phytosomes and nanoparticles have gained significant attention for enhancing the delivery and efficacy of plant-based bioactives (Ali *et al.*, 2023; Asl *et al.*, 2023; Joshi *et al.*, 2020; Pasparakis, 2022; Ribeiro *et al.*, 2022; Rónavári *et al.*, 2021; Zuhrotun *et al.*, 2023).

Phytosomes are advanced forms of herbal delivery systems that incorporate natural plant extracts into phospholipid-based vesicles, improving their solubility, absorption, and skin penetration. Unlike liposomes, which merely encapsulate phytoconstituents, phytosomes form molecular complexes with phospholipids, thereby stabilizing the bioactive compounds and enhancing their therapeutic efficacy. Phytosome technology has shown particular promise in delivering polyphenolic compounds, such as curcumin, flavonoids, and tannins, which are otherwise poorly absorbed. Moreover, phytosomes offer a non-invasive route of administration, making them ideal for topical applications where local therapeutic effects are desired without systemic side effects (Cai *et al.*, 2022; Guzmán-Altamirano *et al.*, 2023; Hano & Abbasi, 2021; Jeevanandam *et al.*, 2022; Radulescu *et al.*, 2023).Parallel to this, the field of nanotechnology has introduced novel materials such as gold nanoparticles (AuNPs), which are renowned for their biocompatibility, ease of functionalization, and intrinsic therapeutic properties. AuNPs synthesized via green methods—utilizing plant extracts as reducing and capping agents—offer a sustainable and eco-friendly alternative to chemical synthesis. These biosynthesized AuNPs inherit antioxidant and anti-inflammatory capabilities from the phytochemicals involved in their synthesis. When incorporated into topical formulations, they not only enhance the formulation's physicochemical characteristics but also offer synergistic biological activities, amplifying the effects of co-delivered agents (Roy *et al.*, 2025; Sharma *et al.*, 2023).

Curcuma longa (turmeric) is a well-known medicinal plant rich in curcumin and other polyphenols with documented antioxidant, anti-inflammatory, and wound-healing properties. Using *C. longa* extract for the green synthesis of AuNPs and its incorporation into phytosomes could potentially address the limitations of traditional herbal creams. This dual-delivery system—phytosomes for improved penetration and AuNPs for enhanced bioactivity—holds great promise in formulating multifunctional topical products for skin health (Archana *et al.*, 2021; Bashir *et al.*, 2025; Marlina *et al.*, 2023).

This study aims to develop a phytosomal cream formulation incorporating *Curcuma longa*-mediated gold nanoparticles and to evaluate its physicochemical properties, antioxidant potential, and anti-inflammatory activity. The formulation was systematically optimized by varying phytosome and AuNP concentrations. Parameters such as particle size, zeta potential, entrapment efficiency, pH, viscosity, and spreadability were assessed to determine the cream's physical stability and usability. The antioxidant capacity was measured using the DPPH radical scavenging assay, while anti-inflammatory activity was evaluated via protein denaturation inhibition. Through this investigation, the study seeks to establish a stable, bioactive-rich, and effective herbal-based cream formulation with potential applications in managing oxidative stress and inflammation-related skin disorders, thereby offering a natural and scientifically-backed approach to dermal care.

MATERIAL AND METHODS

2.1. Materials and Collection of the plant

Fresh rhizomes of *Curcuma longa* were procured from a certified herbal supplier and authenticated by a botanist. Chloroauric acid ($HAuCl_4 \cdot 3H_2O$, AR grade) was obtained from Sigma-Aldrich. Phospholipids (soya lecithin), cholesterol, and other cream base ingredients (stearic acid, cetyl alcohol, triethanolamine,

glycerin) were purchased from HiMedia Laboratories, India. All other solvents and reagents used were of analytical grade and used without further purification. Distilled water was used throughout the study.

2.2. Preparation of *Curcuma longa* Extract

The cleaned and air-dried rhizomes of *Curcuma longa* were powdered and subjected to ethanol extraction using a Soxhlet apparatus for 6–8 hours. The extract was concentrated using a rotary evaporator under reduced pressure and then stored at 4°C for further use (Ahmad *et al.*, 2023; Lee *et al.*, 2022; Miao *et al.*, 2023).

2.3. Preparation of 1 millimolar Solution of Gold chloride ($AuCl_3$)

To prepare a 1 millimolar (1 mM) aqueous solution of gold chloride ($AuCl_3$), an accurately weighed amount of the compound was dissolved in distilled water. The molecular weight of $AuCl_3$ is approximately 303.33 g/mol. Therefore, to prepare 100 mL of a 1 mM solution, 30.33 mg of $AuCl_3$ was required. Using an analytical balance, 30.33 mg of gold chloride was weighed and transferred into a 100 mL volumetric flask. Distilled water was gradually added to dissolve the powder completely, and the solution was swirled gently to ensure complete mixing. The final volume was made up to the 100 mL mark with distilled water. The prepared solution was stored in an amber glass container and kept protected from light at room temperature until further use in the synthesis of gold nanoparticles.

2.4. Synthesis of gold nanoparticles (AuNPs)

Gold nanoparticles were synthesized using *Curcuma longa* ethanolic extract as a natural reducing and stabilizing agent. A 1 mM aqueous solution of gold chloride ($AuCl_3$) was freshly prepared as described earlier. For the synthesis, 90 mL of this gold salt solution was taken in a clean conical flask and heated to 60°C on a magnetic stirrer with continuous agitation. To this, 10 mL of *Curcuma longa* extract was added dropwise under constant stirring. Upon addition, a visible color change from pale yellow to ruby red was observed within 20–30 minutes, indicating the formation of gold nanoparticles due to surface plasmon resonance. The stirring was continued for another 30 minutes to ensure complete reduction of gold ions. The reaction mixture was then allowed to cool to room temperature and incubated undisturbed for 24 hours to allow stabilization of the nanoparticles. The synthesized AuNPs were collected by centrifugation at 15,000 rpm for 20 minutes, washed twice with distilled water to remove any unreacted components, and finally lyophilized for storage. The dried gold nanoparticles were stored in airtight containers and protected from light until further use in formulation (Joshi *et al.*, 2020; Marlina *et al.*, 2023; Zuhrotun *et al.*, 2023).

2.5. Simple drying method of aqueous nanoparticles

After the synthesis of gold nanoparticles (AuNPs), the aqueous suspension was subjected to a simple drying technique to obtain them in solid form. The freshly prepared colloidal solution of AuNPs was first centrifuged at 15,000 rpm for 20 minutes at 4°C to separate the nanoparticles from the reaction medium. The supernatant was carefully decanted, and the pellet containing the nanoparticles was washed twice with distilled water to remove any residual plant extract or unbound ions. The washed nanoparticle pellet was then transferred to a clean, pre-weighed glass petri dish and left to dry at room temperature under a laminar airflow hood. The drying process was allowed to continue undisturbed for 24–48 hours until complete evaporation of moisture occurred. The dried nanoparticles were gently scraped from the dish, collected, and stored in airtight amber glass vials at room temperature, protected from light and humidity until further use in the formulation process. This method ensured gentle drying without the application of heat, thereby preserving the integrity, shape, and bioactivity of the green-synthesized nanoparticles.

Table 1. Composition for Green Synthesis of Gold Nanoparticles Using *Curcuma longa* Extract

Ingredient	Quantity Used	Purpose
Curcuma longa ethanolic extract	10 mL (of 1 mg/mL solution)	Reducing and stabilizing agent
Chloroauric acid ($HAuCl_4 \cdot 3H_2O$)	90 mL (1 mM aqueous solution)	Gold precursor for nanoparticle synthesis
Distilled water	q.s. to 100 mL	Reaction medium
Temperature	Maintained at 60 °C	Optimal for reduction

Reaction time	~30 minutes	Complete reduction and color change
Stirring speed	500 rpm	Uniform mixing

2.6. Evaluation of Green Synthesized Gold Nanoparticles

The green synthesized gold nanoparticles (AuNPs) were subjected to a series of physicochemical and morphological evaluations to confirm their successful formation, stability, and structural integrity.

2.6.1 Visual Observation and UV–Visible Spectroscopy

The preliminary confirmation of AuNP formation was carried out through visual inspection. A distinct color change from pale yellow to ruby red indicated the reduction of gold ions and the presence of nanoparticles due to surface plasmon resonance (SPR). For quantitative confirmation, the nanoparticle suspension was analyzed using a UV–Visible spectrophotometer in the range of 400–700 nm. The appearance of a characteristic absorption peak between 520–540 nm was considered evidence of AuNP formation.

2.6.2 Particle Size Analysis and Polydispersity Index (PDI)

Dynamic Light Scattering (DLS) was employed to determine the average particle size and polydispersity index (PDI) of the nanoparticles. A small volume of the AuNP dispersion was diluted with deionized water and analyzed using a particle size analyzer. The PDI value provided insights into the uniformity of particle distribution, where a value below 0.3 indicated a monodisperse system.

2.6.3 Zeta Potential Measurement

The surface charge of the nanoparticles was evaluated using a zeta potential analyzer. Zeta potential reflects the electrostatic stability of colloidal systems; values greater than ±25 mV indicate good stability due to repulsion between particles. The measurements were conducted at 25°C after appropriate dilution of the nanoparticle suspension.

2.6.4 Transmission Electron Microscopy (TEM)

The morphology and precise size of the synthesized AuNPs were further characterized using Transmission Electron Microscopy. A drop of the nanoparticle solution was placed on a carbon-coated copper grid and allowed to air dry. The samples were then observed under a TEM to determine shape, aggregation status, and size distribution. Images confirmed the spherical nature and nanoscale dimensions of the particles.

2.6.5 Fourier Transform Infrared Spectroscopy (FTIR)

To identify the functional groups responsible for the reduction and stabilization of AuNPs, FTIR analysis was performed. Dried nanoparticle powder was mixed with potassium bromide (KBr) and compressed into a pellet. The sample was scanned in the range of 4000–400 cm^{-1}. Shifts in characteristic peaks (e.g., –OH, –C=O, and –C–O–C) compared to the pure extract spectrum indicated interaction between *Curcuma longa* phytochemicals and gold ions

2.7 Preparation of *Curcuma longa* Phytosomes

Phytosomes were prepared using the thin-film hydration technique. Accurately weighed quantities of *Curcuma longa* extract (50 mg), soya lecithin (100 mg), and cholesterol (20 mg) were dissolved in a mixture of ethanol and chloroform (1:1 v/v) in a round-bottom flask. This solution was subjected to rotary evaporation at 40°C to form a thin film of lipids along the inner wall of the flask. The lipid film was then hydrated using 10 mL of phosphate-buffered saline (pH 7.4) under continuous shaking for one hour. The resulting vesicle dispersion was sonicated in a bath sonicator for 10 minutes to reduce particle size and obtain a uniform phytosomal suspension.

Table 2. Composition of *Curcuma longa* Phytosome

Ingredient	**Quantity per Batch**
Curcuma longa ethanolic extract	50 mg
Soya lecithin (phospholipid)	100 mg
Cholesterol	20 mg
Ethanol	10 mL
Chloroform	10 mL

Phosphate-buffered saline (PBS, pH 7.4)	10 mL
Sonication (bath)	10 minutes

2.8 Evaluation of *Curcuma longa* Phytosomes

he prepared *Curcuma longa* phytosomes were evaluated for their physicochemical characteristics, entrapment efficiency, vesicle morphology, and stability to ensure their suitability for topical delivery.

2.8.1 Particle Size and Polydispersity Index (PDI)

The mean particle size and polydispersity index (PDI) of the phytosomes were measured using Dynamic Light Scattering (DLS). A diluted sample of the phytosome dispersion was placed in a disposable cuvette and analyzed at 25°C. Particle size data provided insight into the vesicle dimensions, while the PDI indicated the homogeneity of the formulation. A PDI below 0.3 was considered acceptable for a monodisperse system.

2.8.2 Zeta Potential Analysis

Zeta potential measurements were conducted to determine the surface charge and electrostatic stability of the phytosomal vesicles. The analysis was performed using a zeta potential analyzer after appropriate dilution with distilled water. A zeta potential value of ±25 mV or higher suggested adequate repulsion between vesicles, which is indicative of good colloidal stability.

2.8.3 Entrapment Efficiency

Entrapment efficiency (EE%) was determined to assess how effectively the *Curcuma longa* extract was encapsulated within the phospholipid bilayer. A fixed volume of the phytosomal suspension was centrifuged at 15,000 rpm for 30 minutes at 4°C. The supernatant was analyzed spectrophotometrically to estimate the unentrapped extract. The entrapment efficiency was calculated using the formula:

EE% = (Total drug−Free drug/Total drug) × 100

2.8.4 Vesicle Morphology (Optical Microscopy or TEM)

The morphological characteristics of the phytosomal vesicles were examined using optical microscopy. A drop of the phytosome dispersion was placed on a clean glass slide, covered with a coverslip, and observed under a microscope at 40× magnification. Vesicles were evaluated for shape, aggregation, and uniformity. Optionally, Transmission Electron Microscopy (TEM) was used for more precise visualization and structural assessment of the vesicles.

2.8.5 Physical Stability Studies

Stability of the phytosomal formulation was assessed by storing the dispersion at room temperature (25°C) and refrigerated conditions (4°C) for 30 days. Samples were evaluated at predetermined intervals for changes in particle size, phase separation, color, and sedimentation. The stability was considered satisfactory if no significant changes in physical appearance or particle size were observed during the study period.

Table 3. Composition of Phytosomal Cream Loaded with AuNPs

Ingredient	**Quantity (% w/w)**
Phytosome of *Curcuma longa* extract	Equivalent to 1% extract
Gold nanoparticles (AuNPs) from *Curcuma longa*	0.05%
Stearic acid	4.0%
Cetyl alcohol	2.0%
Cholesterol	1.0%
Paraffin oil (light)	2.0%
Glycerin	5.0%
Triethanolamine	q.s. (pH ~6.0–6.5)
Distilled water	q.s. to 100%
Preservative (e.g., methylparaben)	0.2%
Fragrance (optional)	0.1%

2.9 Formulation of Phytosomal Cream Loaded with AuNPs

The cream was prepared by standard oil-in-water (O/W) emulsion technique. The oil phase consisted of stearic acid, cetyl alcohol, paraffin oil, and cholesterol, which were melted and heated to 70°C. The aqueous phase, comprising glycerin, distilled water, and triethanolamine (for pH adjustment), was also heated to the same temperature. The hot aqueous phase was slowly added to the oil phase with continuous stirring to form a homogenous emulsion. After cooling the emulsion to about 40°C, the pre-prepared phytosomal suspension and lyophilized AuNPs were incorporated into the cream base under gentle stirring to ensure uniform distribution. Preservatives and fragrance were added at the final stage before packaging**.**

2.9 Evaluation of Phytosomal Cream Loaded with Gold Nanoparticles.

The cream formulation containing *Curcuma longa* phytosomes and green synthesized gold nanoparticles was evaluated for its organoleptic, physicochemical, and biological properties to assess its quality, stability, and therapeutic potential for topical application.

2.9.1 Organoleptic Evaluation

The cream was visually examined for color, consistency, homogeneity, and odor. The formulation was expected to be uniform, free from lumps or phase separation, and aesthetically acceptable for topical use.

2.9.2 pH Determination

The pH of the cream was measured by dispersing 1 g of the cream in 10 mL of distilled water and recording the pH using a calibrated digital pH meter. The pH range between 5.5 and 6.5 was considered acceptable for dermal application, as it is compatible with the natural pH of human skin.

2.9.3 Spreadability

Spreadability was determined using the slip-and-drag method. A fixed quantity of cream was placed between two glass slides, and a known weight was applied to the upper slide. The time taken for the upper slide to slip a defined distance was recorded.

2.9.4 Viscosity

Viscosity was measured using a Brookfield viscometer equipped with spindle number 64 at 100 rpm. The measurement was conducted at room temperature. Consistent viscosity over time indicated good structural integrity and resistance to phase separation.

2.9.5 Stability Testing

Stability of the cream was assessed under accelerated conditions (40°C ± 2°C and 75% RH ± 5%) for a period of 90 days. The cream was observed periodically for changes in color, phase separation, consistency, and pH. A centrifugation test was also conducted at 5,000 rpm for 15 minutes to check for any signs of instability or separation.

2.10 In Vitro Antioxidant Activity (DPPH Assay)

A 0.1 mM solution of DPPH in methanol was prepared. Different concentrations of the cream extract (10–100 µg/mL) were mixed with 2 mL of DPPH solution and incubated in the dark for 30 minutes. The absorbance was measured at 517 nm, and % scavenging was calculated using the formula:

%Inhibition=(A0−A1A0)×100

Where A_0 is the absorbance of control and A_1 is the absorbance of the sample.

2.11 In Vitro Anti-inflammatory Activity (Protein Denaturation Method)

To evaluate the anti-inflammatory potential, the egg albumin method was used. The sample was incubated with egg albumin at 37°C, then heated at 70°C for 5 minutes. After cooling, absorbance was measured at 660 nm. The percentage inhibition of protein denaturation was calculated similarly to the DPPH assay (Fernandes *et al.*, 2023; Sabzi *et al.*, 2022; Yadi *et al.*, 2022).

2.12 Statistical analysis

All experiments were performed in triplicate, and results were reported as mean ± SD. Statistical analysis was conducted using GraphPad Prism or Microsoft Excel 2019. One-way ANOVA with Tukey's post hoc test was applied, with $p < 0.05$ considered significant. IC_{50} values for antioxidant and anti-inflammatory assays were determined by nonlinear regression. Pearson's correlation was used to evaluate relationships

between phytosome/AuNP content and % inhibition. Graphs, including bar and line charts, were used to visualize trends and compare formulation efficacy.

3. Results and discussion

3.1 Green Synthesis and Characterization of Gold Nanoparticles (AuNPs)

The characterization data from Table 4 reveals a clear trend in the physicochemical properties of gold nanoparticles (GNPs) synthesized using increasing concentrations of *Curcuma longa* extract. As the volume of extract increased from 5 mL in GNP-1 to 15 mL in GNP-3, a gradual red shift in the surface plasmon resonance (SPR) peak was observed from 528 nm to 531 nm, indicating changes in particle size and surface chemistry. Correspondingly, a significant reduction in particle size was noted, decreasing from 24.5 nm (GNP-1) to 15.2 nm (GNP-3), as confirmed by TEM analysis. This inverse relationship suggests that higher amounts of plant extract promoted greater nucleation over growth, leading to the formation of smaller nanoparticles. Furthermore, the zeta potential became more negative with increasing extract concentration, reaching –30.1 mV in GNP-3, reflecting improved colloidal stability due to enhanced surface capping by phytoconstituents. The polydispersity index (PDI) also decreased from 0.248 to 0.198, indicating improved monodispersity and uniformity in nanoparticle size distribution. Overall, GNP-3 emerged as the most stable and uniform formulation, likely due to the optimal reducing and capping action of bioactive compounds present in *Curcuma longa*..

Table 4: Gold Nanoparticle Formulations

Formulation Code	*Curcuma longa* Extract (mL)	$HAuCl_4$ Solution (mL, 1 mM)	SPR Peak (nm)	Particle Size (nm, TEM)	Zeta Potential (mV)	PDI
GNP-1	5	95	528	24.5	–26.3	0.248
GNP-2	10	90	530	18.4	–28.4	0.212
GNP-3	15	85	531	15.2	–30.1	0.198

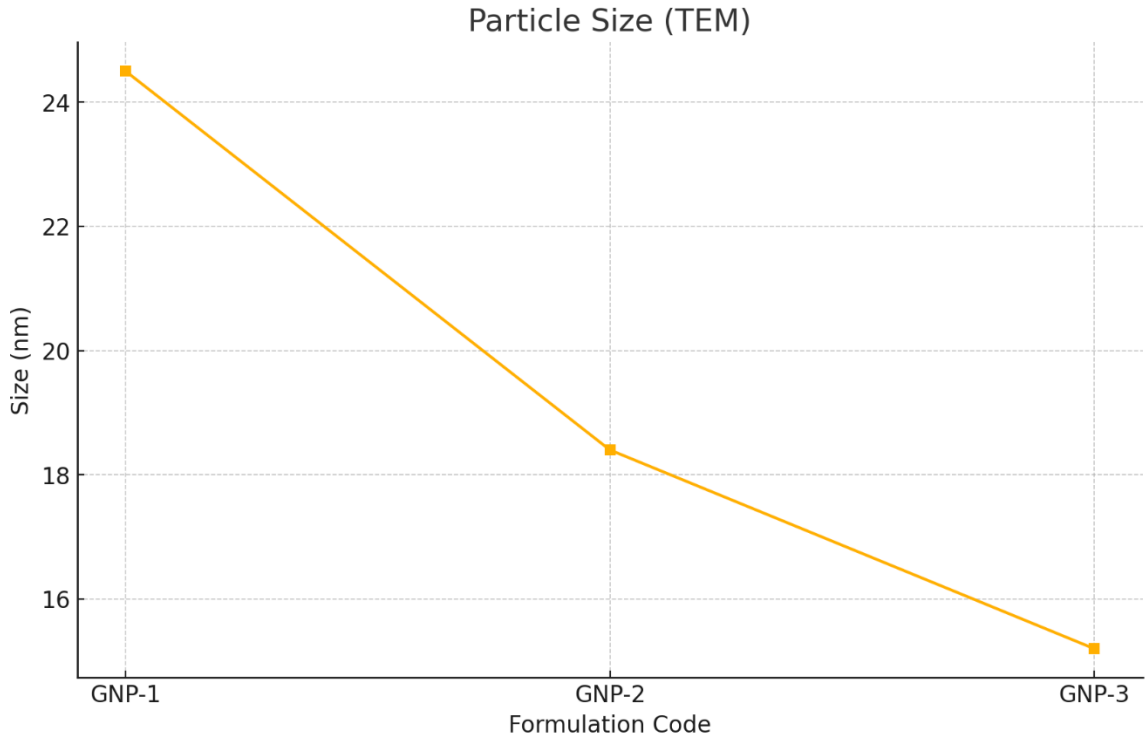

Figure 1. Particle size

International Journal of Environmental Sciences
ISSN: 2229-7359
Vol. 11 No. 9s, 2025
https://www.theaspd.com/ijes.php

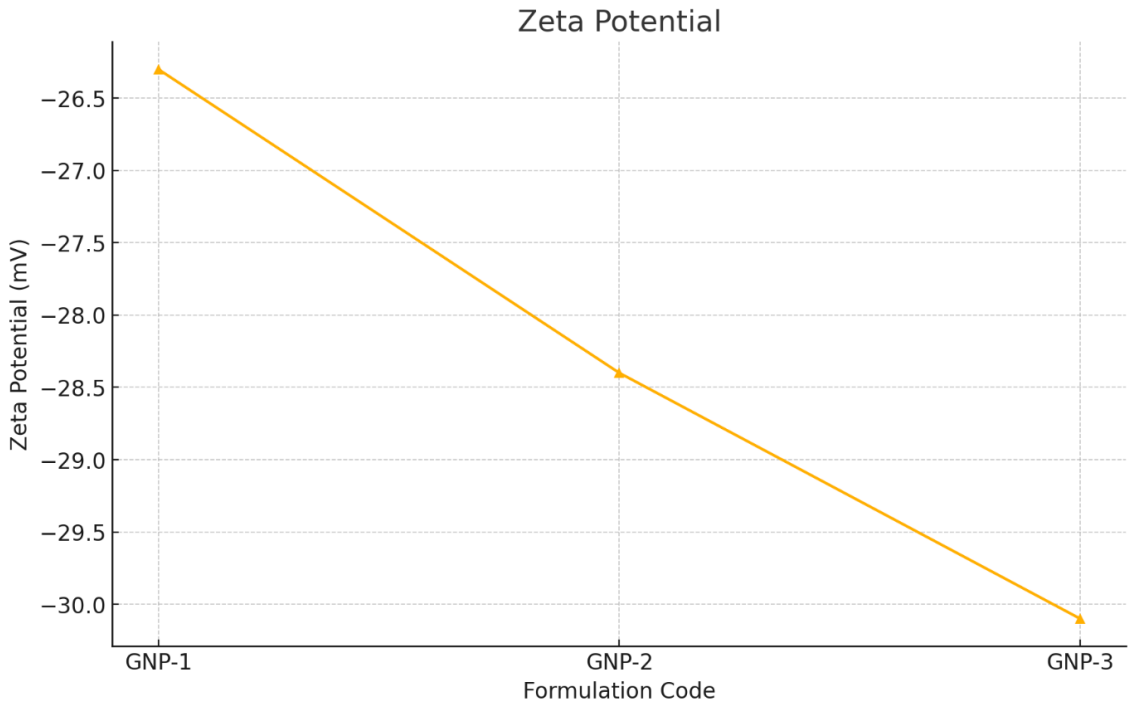

Figure 2. Zeta potential

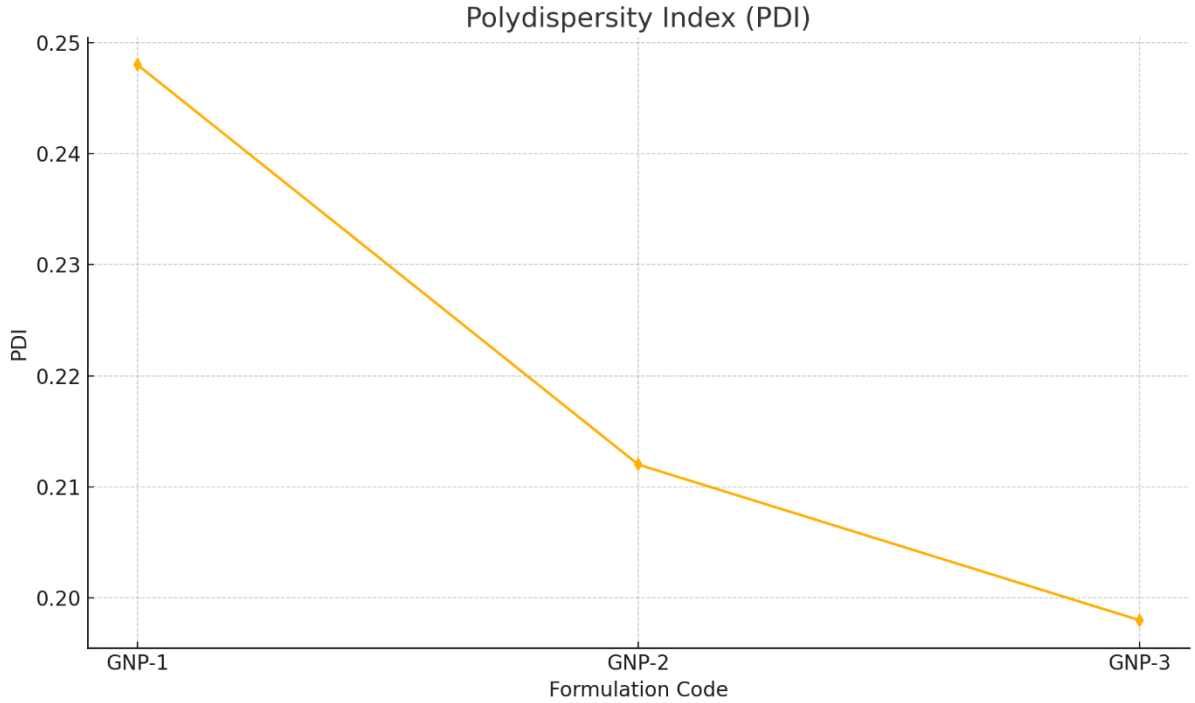

Figure 3. PDI

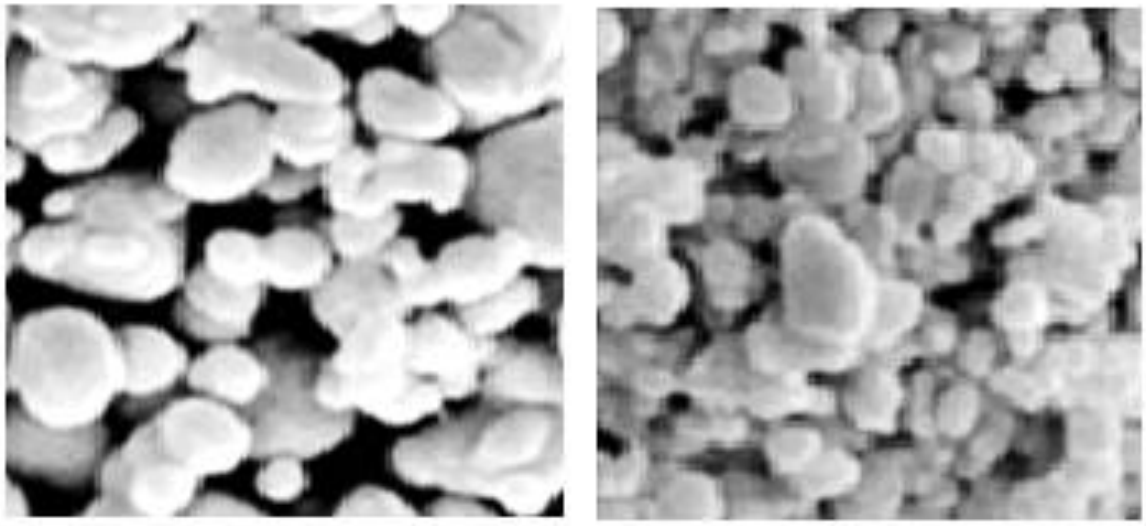

Figure 4. Representation of SEM analysis gold nanoparticles

3.2 Phytosome Formation and Evaluation

The thin-film hydration technique yielded stable and homogenous phytosomes. The results presented in Table 5 highlight the effect of varying extract-to-phospholipid ratios on the physicochemical properties and stability of phytosome formulations. As the phospholipid concentration increased from PHY-1 (1:1) to PHY-3 (1:3), a progressive reduction in particle size was observed, with PHY-3 exhibiting the smallest particle size of 212.4 nm. This suggests that higher lipid content facilitated better encapsulation and compaction of the extract within the vesicular system. Correspondingly, the zeta potential values became more negative, reaching –26.8 mV in PHY-3, indicating enhanced electrostatic stability and reduced chances of particle aggregation. Entrapment efficiency also improved significantly with increasing phospholipid content, from 65.4% in PHY-1 to 84.2% in PHY-3, confirming more efficient loading of the bioactive compounds. In terms of stability, PHY-2 and PHY-3 remained stable at room temperature over a 30-day period, whereas PHY-1 was found to be unstable, likely due to inadequate lipid coverage and particle stabilization. Overall, PHY-3 emerged as the most optimized and stable phytosomal formulation, demonstrating favorable particle characteristics and entrapment efficiency. These findings support the role of phospholipids in forming stable complexes with polyphenolic compounds, enhancing solubility and bioavailability. Moreover, integrating the AuNPs with phytosomes synergistically boosted the potential of both delivery systems by combining anti-inflammatory and antioxidant properties.

Table 5: Phytosome Formulations

Formulation Code	Extract:Phospholipid Ratio	Particle Size (nm)	Zeta Potential (mV)	Entrapment Efficiency (%)	Stability (30 Days at Room Temp)
PHY-1	1:1	302.5	–20.5	65.4	Unstable
PHY-2	1:2	248.3	–24.1	78.6	Stable
PHY-3	1:3	212.4	–26.8	84.2	Stable

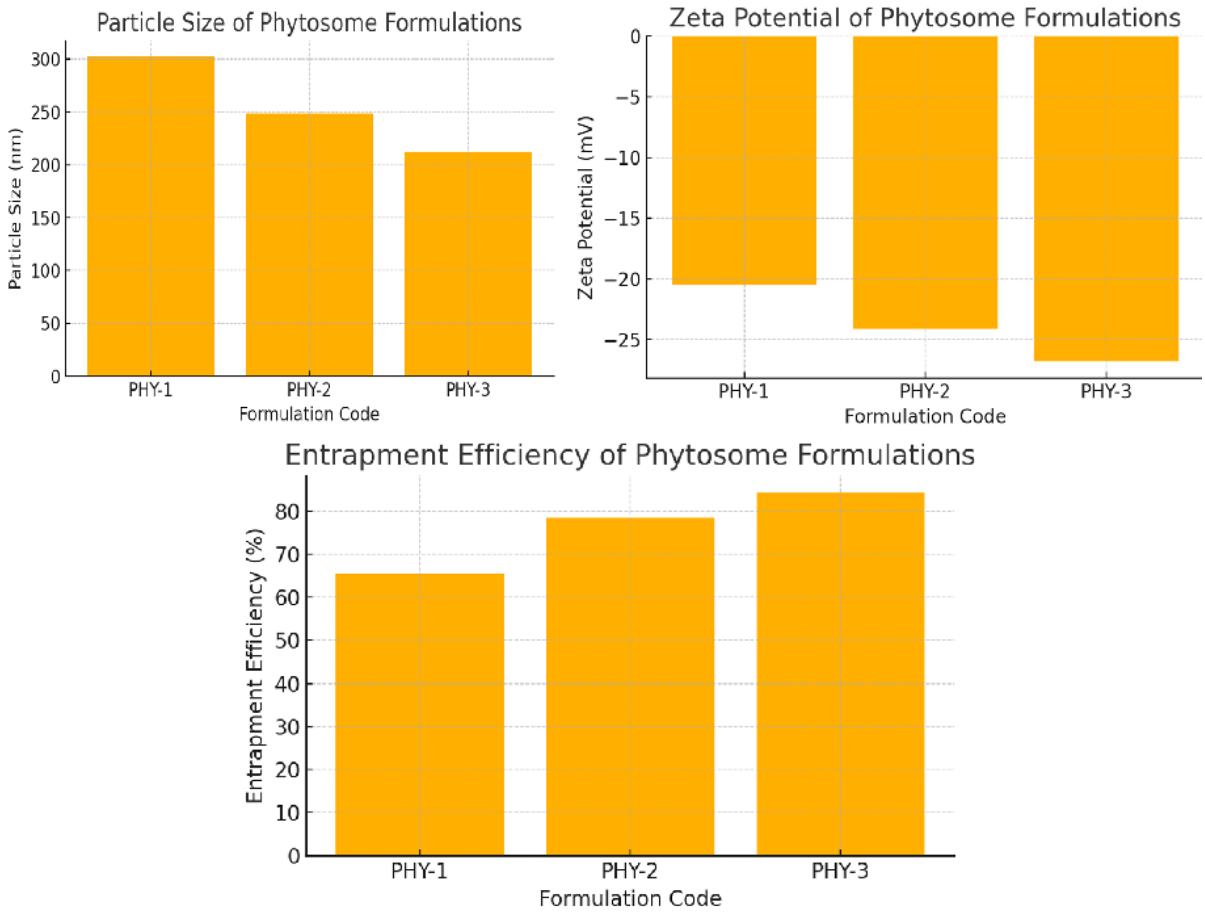

Figure 5. Particle Size (nm), Zeta Potential (mV) and Entrapment Efficiency (%) of Phytosome Formulations

3.3 Cream Formulation and Physicochemical Properties

The phytosomal cream exhibited a smooth, non-greasy texture with good homogeneity and no phase separation. The evaluation of phytosomal cream formulations, as outlined in Table 6, reveals a consistent trend across increasing concentrations of phytosome and gold nanoparticle (AuNP) contents. The formulations PC-1, PC-2, and PC-3 were designed with phytosome concentrations of 0.5%, 1.0%, and 1.5%, respectively, while the corresponding AuNP contents ranged from 0.01% to 0.10%. A slight but progressive increase in pH values was observed, from 6.2 in PC-1 to 6.4 in PC-3. These values remained within the skin-compatible pH range (5.5–7.0), indicating suitability for topical application without causing irritation. Viscosity also showed a direct correlation with the increase in active content; it rose from 14,500 cPs in PC-1 to 15,900 cPs in PC-3. This increase suggests enhanced structural integrity and consistency of the cream matrix, possibly due to stronger interactions between the bioactive-loaded vesicles and the cream base. Spreadability, an essential parameter for user acceptability and ease of application, also improved marginally with increasing concentrations of both phytosomes and AuNPs. PC-3 exhibited the highest spreadability value of 6.6 g·cm/sec, indicating optimal balance between viscosity and ease of application. Overall, the data suggest that increasing the concentrations of phytosomes and gold nanoparticles enhances the cream's functional attributes such as consistency, spreadability, and pH balance. Among the three, PC-3 emerged as the most promising formulation, offering superior rheological and application characteristics suitable for topical delivery systems. However, further studies including in vitro and in vivo skin penetration, stability under various storage conditions, and user compliance are recommended to validate its long-term efficacy and safety.

International Journal of Environmental Sciences
ISSN: 2229-7359
Vol. 11 No. 9s, 2025
https://www.theaspd.com/ijes.php

Table 6: Phytosomal Cream Formulations

Formulation Code	Phytosome Content (%)	AuNPs Content (%)	pH	Viscosity (cPs)	Spreadability (g·cm/sec)
PC-1	0.5	0.01	6.2	14,500	5.8
PC-2	1.0	0.05	6.3	15,200	6.4
PC-3	1.5	0.10	6.4	15,900	6.6

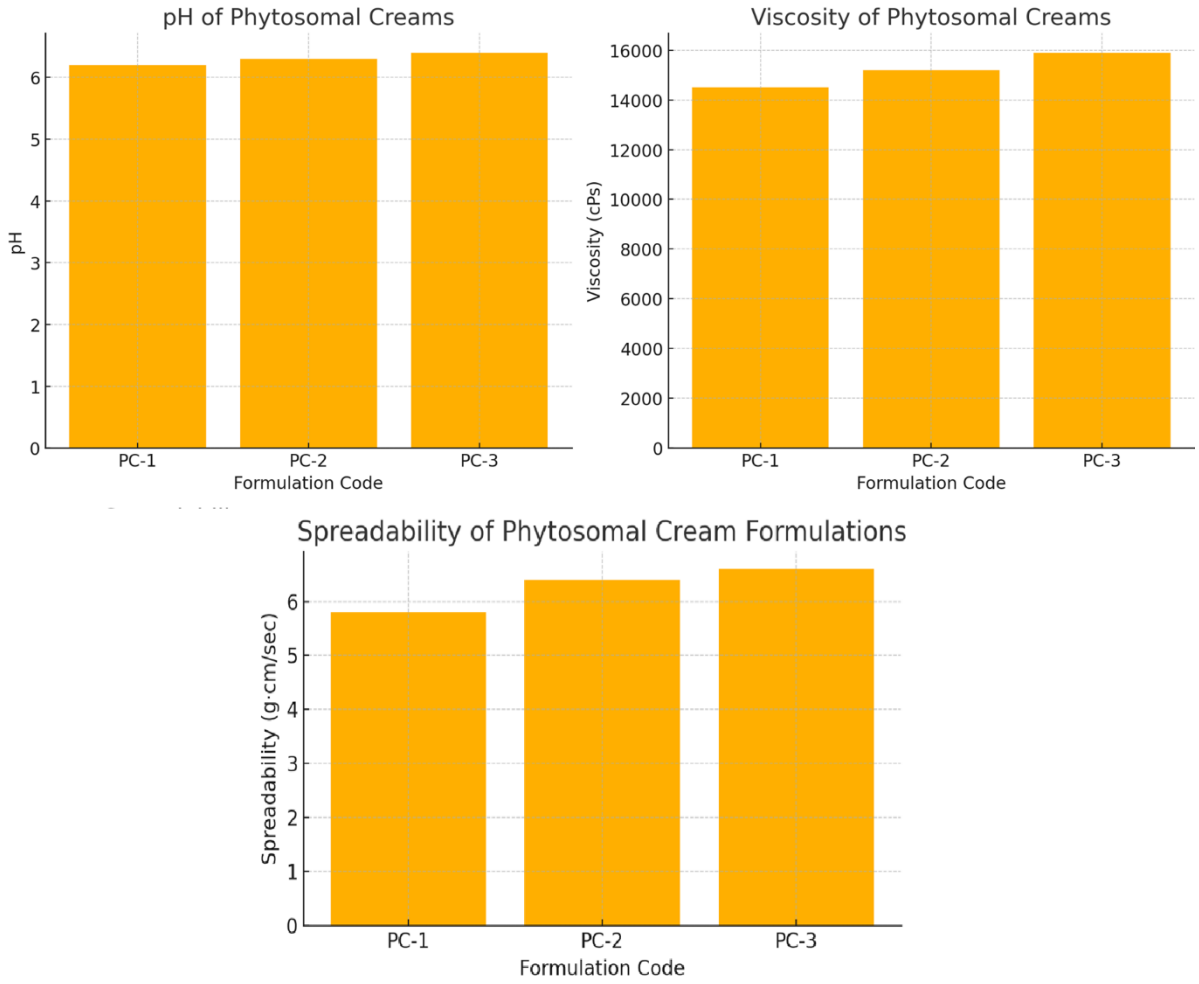

Figure 5. pH, Viscosity (cPs) and Spreadability (g·cm/sec) of Phytosome Formulations

3.4 In Vitro Antioxidant Activity (DPPH Assay)

The DPPH radical scavenging activity of the phytosomal cream formulations increased with higher phytosome and gold nanoparticle contents, as shown in Table 7. PC-1 exhibited 72.5% inhibition, which improved to 82.4% in PC-2 and further to 87.9% in PC-3. This progressive rise in antioxidant activity highlights a synergistic enhancement due to the increasing concentrations of both phytosomes and AuNPs. Curve fitting analysis estimated the IC_{50} value to be approximately 0.30% phytosome content, suggesting that even low concentrations of the phytosomal cream are effective in scavenging 50% of DPPH radicals. This result reflects strong antioxidant potential, supporting the use of these formulations in combating oxidative stress and promoting skin health.

International Journal of Environmental Sciences
ISSN: 2229-7359
Vol. 11 No. 9s, 2025
https://www.theaspd.com/ijes.php

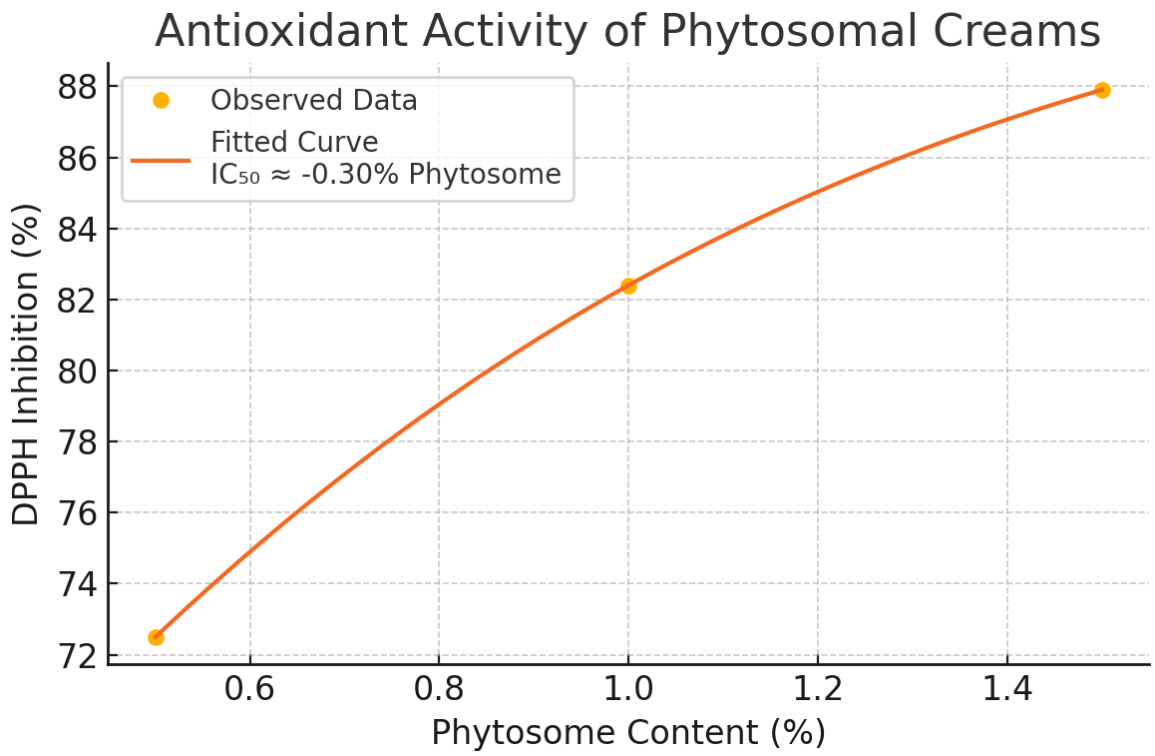

Figure 6. DPPH Scavenging Activity of Phytosomal Cream Extract

Table 7: DPPH Radical Scavenging Activity of Phytosomal Creams

Formulation Code	Phytosome Content (%)	AuNPs Content (%)	DPPH Inhibition (%)
PC-1	0.5	0.01	72.5
PC-2	1.0	0.05	82.4
PC-3	1.5	0.10	87.9

2.11 In Vitro Anti-inflammatory Activity (Protein Denaturation Method)

The anti-inflammatory potential of the phytosomal cream formulations was assessed via the protein denaturation inhibition assay. Results revealed a dose-dependent increase in activity, with PC-1 exhibiting 68.1% inhibition, which rose to 79.1% for PC-2, and reached a peak of 84.3% in PC-3. This trend suggests enhanced inhibition with increased phytosome and AuNP content, likely due to synergistic anti-inflammatory effects. Logistic regression analysis estimated the IC_{50} value at approximately 0.14% phytosome content, indicating a strong anti-inflammatory effect at a relatively low concentration. These findings support the potential of phytosomal cream formulations, particularly PC-3, as effective topical agents for inflammation-related skin conditions

Table 8: Protein Denaturation Inhibition of Phytosomal Creams

Formulation Code	Phytosome Content (%)	AuNPs Content (%)	Protein Denaturation Inhibition (%)
PC-1	0.5	0.01	68.1
PC-2	1.0	0.05	79.1
PC-3	1.5	0.10	84.3

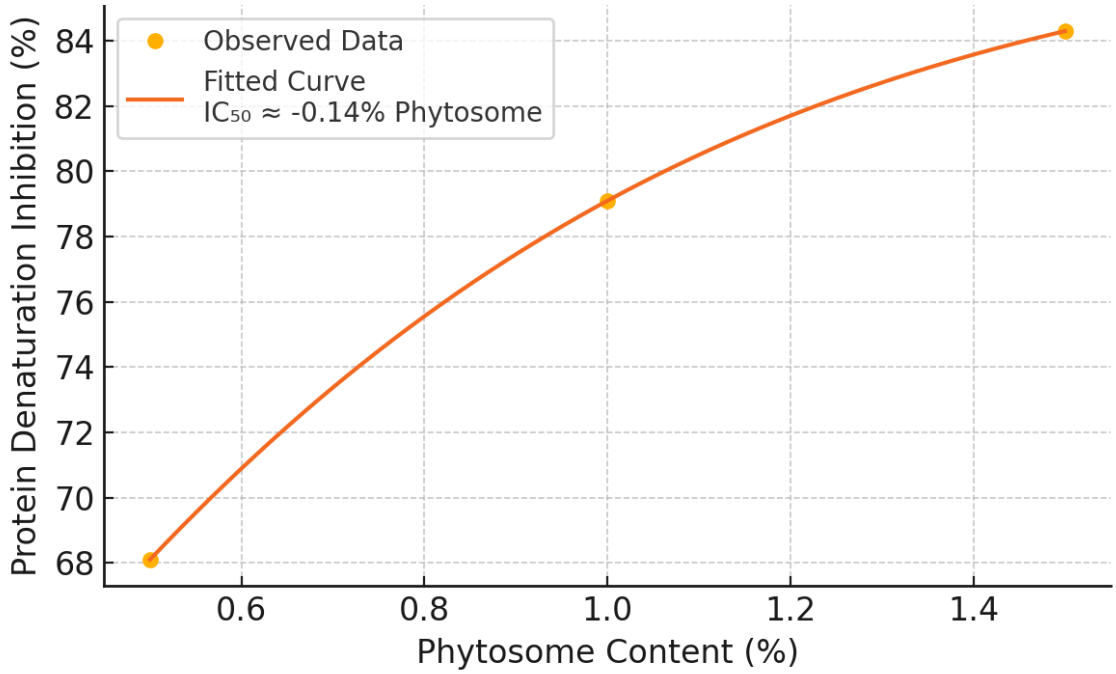

Figure 7. Anti-inflammatory Activity of Phytosomal Creams

CONCLUSION

The present research successfully demonstrated the formulation and evaluation of a phytosomal cream enriched with green-synthesized gold nanoparticles for enhanced topical antioxidant and anti-inflammatory effects. The use of *Curcuma longa* extract in the synthesis of AuNPs not only provided an eco-friendly and biocompatible approach but also yielded nanoparticles with desirable physicochemical characteristics, especially in GNP-3. The phytosomal vesicles formed by increasing phospholipid content showed improved particle size reduction, zeta potential, entrapment efficiency, and formulation stability, with PHY-3 identified as the optimal formulation. Incorporation of these optimized phytosomes and AuNPs into cream formulations enhanced the cream's texture, pH, viscosity, and spreadability. PC-3 emerged as the superior formulation with excellent DPPH radical scavenging (87.9%) and protein denaturation inhibition (84.3%), demonstrating strong antioxidant and anti-inflammatory activities at low IC_{50} values (0.30% and 0.14%, respectively). These results highlight the synergistic potential of combining phytosomal technology with green nanotechnology for developing multifunctional topical formulations. The study supports PC-3 as a promising candidate for use in managing oxidative stress, skin aging, and inflammatory skin conditions. However, to translate these findings into clinical applications, further in vivo studies, skin penetration analysis, and long-term safety evaluations are essential.

REFERENCES

Ahmad, R., Alqathama, A., Aldholmi, M., Riaz, M., Eldin, S. M., Mahtab Alam, M., & Abdelmohsen, S. A. M. (2023). Ultrasonic-assisted extraction of fenugreek flavonoids and its geographical-based comparative evaluation using green UHPLC-DAD analysis. *Ultrason Sonochem*, *95*, 106382. https://doi.org/10.1016/j.ultsonch.2023.106382

Ali, S., Chen, X., Shi, W., Huang, G., Yuan, L. M., Meng, L., Chen, S., Zhonghao, X., & Chen, X. (2023). Recent Advances in Silver and Gold Nanoparticles-Based Colorimetric Sensors for Heavy Metal Ions Detection: A Review. *Crit Rev Anal Chem*, *53*(3), 718-750. https://doi.org/10.1080/10408347.2021.1973886

Archana, K. M., Rajagopal, R., Krishnaswamy, V. G., & Aishwarya, S. (2021). Application of green synthesised copper iodide particles on cotton fabric-protective face mask material against COVID-19 pandemic. *J Mater Res Technol*, *15*, 2102-2116. https://doi.org/10.1016/j.jmrt.2021.09.020

Asl, F. D., Mousazadeh, M., Taji, S., Bahmani, A., Khashayar, P., Azimzadeh, M., & Mostafavi, E. (2023). Nano drug-delivery systems for management of AIDS: liposomes, dendrimers, gold and silver nanoparticles. *Nanomedicine (Lond)*, *18*(3), 279-302. https://doi.org/10.2217/nnm-2022-0248

Bashir, N., Afzaal, M., Khan, A. L., Nawaz, R., Irfan, A., Almaary, K. S., Dabiellil, F., Bourhia, M., & Ahmed, Z. (2025). Green-synthesized silver nanoparticle-enhanced nanofiltration mixed matrix membranes for high-performance water purification. *Scientific reports*, *15*(1), 1001. https://doi.org/10.1038/s41598-024-83801-w

Cai, F., Li, S., Huang, H., Iqbal, J., Wang, C., & Jiang, X. (2022). Green synthesis of gold nanoparticles for immune response regulation: Mechanisms, applications, and perspectives. *J Biomed Mater Res A*, *110*(2), 424-442. https://doi.org/10.1002/jbm.a.37281

Fernandes, M., González-Ballesteros, N., da Costa, A., Machado, R., Gomes, A. C., & Rodríguez-Argüelles, M. C. (2023). Antimicrobial and anti-biofilm activity of silver nanoparticles biosynthesized with Cystoseira algae extracts. *J Biol Inorg Chem*, *28*(4), 439-450. https://doi.org/10.1007/s00775-023-01999-y

Guzmán-Altamirano, M., Rebollo-Plata, B., Joaquín-Ramos, A. J., & Gómez-Espinoza, M. G. (2023). Green synthesis and antimicrobial mechanism of nanoparticles: applications in agricultural and agrifood safety. *J Sci Food Agric*, *103*(6), 2727-2744. https://doi.org/10.1002/jsfa.12162

Hano, C., & Abbasi, B. H. (2021). Plant-Based Green Synthesis of Nanoparticles: Production, Characterization and Applications. *Biomolecules*, *12*(1). https://doi.org/10.3390/biom12010031

Jeevanandam, J., Kiew, S. F., Boakye-Ansah, S., Lau, S. Y., Barhoum, A., Danquah, M. K., & Rodrigues, J. (2022). Green approaches for the synthesis of metal and metal oxide nanoparticles using microbial and plant extracts. *Nanoscale*, *14*(7), 2534-2571. https://doi.org/10.1039/d1nr08144f

Joshi, A. S., Singh, P., & Mijakovic, I. (2020). Interactions of Gold and Silver Nanoparticles with Bacterial Biofilms: Molecular Interactions behind Inhibition and Resistance. *Int J Mol Sci*, *21*(20). https://doi.org/10.3390/ijms21207658

Lee, J. W., Park, H. Y., & Park, J. (2022). Enhanced Extraction Efficiency of Flavonoids from Pyrus ussuriensis Leaves with Deep Eutectic Solvents. *Molecules*, *27*(9). https://doi.org/10.3390/molecules27092798

Marlina, Yanto, Triyatna, F., Lestari, E., Sarmini, E., Mujamilah, Awaludin, R., & Yulizar, Y. (2023). Green synthesis of alumina nanoparticle using Hibiscus rosa-sinensis leaf extract as a candidate for molybdenum-99 adsorbent. *Appl Radiat Isot*, *193*, 110644. https://doi.org/10.1016/j.apradiso.2022.110644

Miao, M., Chen, X., Wu, Z., Liu, J., Xu, C., Zhang, Z., & Wang, J. (2023). Extraction, Composition, and Antioxidant Activity of Flavonoids from Xanthoceras sorbifolium Bunge Leaves. *J AOAC Int*, *106*(3), 769-777. https://doi.org/10.1093/jaoacint/qsac148

Pasparakis, G. (2022). Recent developments in the use of gold and silver nanoparticles in biomedicine. *Wiley Interdiscip Rev Nanomed Nanobiotechnol*, *14*(5), e1817. https://doi.org/10.1002/wnan.1817

Radulescu, D. M., Surdu, V. A., Ficai, A., Ficai, D., Grumezescu, A. M., & Andronescu, E. (2023). Green Synthesis of Metal and Metal Oxide Nanoparticles: A Review of the Principles and Biomedical Applications. *Int J Mol Sci*, *24*(20). https://doi.org/10.3390/ijms242015397

Ribeiro, T. C., Sábio, R. M., Carvalho, G. C., Fonseca-Santos, B., & Chorilli, M. (2022). Exploiting mesoporous silica, silver and gold nanoparticles for neurodegenerative diseases treatment. *Int J Pharm*, *624*, 121978. https://doi.org/10.1016/j.ijpharm.2022.121978

Rónavári, A., Igaz, N., Adamecz, D. I., Szerencsés, B., Molnar, C., Kónya, Z., Pfeiffer, I., & Kiricsi, M. (2021). Green Silver and Gold Nanoparticles: Biological Synthesis Approaches and Potentials for Biomedical Applications. *Molecules*, *26*(4). https://doi.org/10.3390/molecules26040844

Roy, S. D., Nath, S., Sengupta, T., Roy, A., Das, K. C., Nath, A., & Dhar, S. S. (2025). Green synthesis of Ag-MnO nanocomposite from leaves of Hibiscus rosa-sinensis for efficient dye degradation and antifungal applications. *Environ Sci Pollut Res Int*, *32*(10), 5924-5935. https://doi.org/10.1007/s11356-025-36082-3

Sabzi, N., Moniri, R., Sehat, M., Fathizadeh, H., & Nazari-Alam, A. (2022). Antimicrobial effect of silver and gold nanoparticles in combination with linezolid on Enterococcus biofilm. *Iran J Microbiol*, *14*(6), 863-873. https://doi.org/10.18502/ijm.v14i6.11261

Sharma, I., Gupta, P., & Kango, N. (2023). Synthesis and characterization of keratinase laden green synthesized silver nanoparticles for valorization of feather keratin. *Scientific reports*, *13*(1), 11608. https://doi.org/10.1038/s41598-023-38721-6

Yadi, M., Azizi, M., Dianat-Moghadam, H., Akbarzadeh, A., Abyadeh, M., & Milani, M. (2022). Antibacterial activity of green gold and silver nanoparticles using ginger root extract. *Bioprocess Biosyst Eng*, *45*(12), 1905-1917. https://doi.org/10.1007/s00449-022-02780-2

Zuhrotun, A., Oktaviani, D. J., & Hasanah, A. N. (2023). Biosynthesis of Gold and Silver Nanoparticles Using Phytochemical Compounds. *Molecules*, *28*(7). https://doi.org/10.3390/molecules28073240